Inorganic Chemistry
Article

Inorg. Chem. **2010**, *49*, 595–605 **595**
DOI: 10.1021/ic901911h

A Multifrequency High-Field Electron Paramagnetic Resonance Study of $Co^{II}S_4$ Coordination

Dimitrios Maganas,[†] Sergey Milikisyants,[‡] Jorrit M. A. Rijnbeek,[‡] Silvia Sottini,[‡] Nikolaos Levesanos,[†] Panayotis Kyritsis,*[,†] and Edgar J. J. Groenen*[,‡]

[†]*Inorganic Chemistry Laboratory, Department of Chemistry, National and Kapodistrian University of Athens, GR-15771 Athens, Greece and* [‡]*Department of Molecular Physics, Huygens Laboratory, Leiden University, PO Box 9504, 2300 RA Leiden, The Netherlands*

Received September 28, 2009

Advanced electron paramagnetic resonance (EPR) methods have been employed in the study of two high-spin cobalt(II) complexes, $Co[(SPPh_2)_2N]_2$ ($Co^{Ph,Ph}L_2$) and $Co[(SPPh_2)(SP^iPr_2)N]_2$ ($Co^{iPr,Ph}L_2$), in which the bidentate disulfidoimidodiphosphinato ligands make up for a pseudotetrahedral sulfur coordination of the transition metal. The CoS_4 core in the two complexes has slightly different structure, owing to the different peripheral groups (phenyl or isopropyl) bound to the phosphorus atoms. To determine the zero-field splitting, notoriously difficult for high-spin cobalt(II), the two complexes required different approaches. For $Co^{Ph,Ph}L_2$, the study of the X-band EPR spectrum of a single crystal as a function of temperature revealed a nearly axial character of the zero-field splitting (ZFS; $E/D \approx -0.05$). For $Co^{iPr,Ph}L_2$, the combination of the EPR spectra at 9, 95, and 275 GHz revealed a rhombic character of the ZFS ($E/D \approx -0.33$). The energy difference between the Kramers doublets in $Co^{Ph,Ph}L_2$ and $Co^{iPr,Ph}L_2$ amounts to 24 cm^{-1} and 30 cm^{-1}, respectively. From the X-band EPR spectra of diamagnetically diluted single crystals at fields up to 2.5 T for $Co^{Ph,Ph}L_2$ and 0.5 T for $Co^{iPr,Ph}L_2$, the effective g tensors and cobalt hyperfine tensors have been determined, including the direction of the principal axes in the cobalt sites. The values of the EPR observables are discussed in relation to the structural characteristics of the first (CoS_4) and second coordination sphere in the complexes.

Introduction

The biological chemistry of Co is not as extensive compared to other first transition series elements, such as Mn, Fe, Cu and Zn. It has been postulated that acid−base catalysis in hydrolytic reactions by biological Co-active sites would not offer distinctive advantages compared to Zn-active sites, whereas biological redox reactions could be well performed by the most accessible biological elements Mn, Fe, and Cu.[1] The most easily recognized biological activity of Co is its organometallic active site in vitamin B_{12} and related systems.[2−4]

However, extensive work over the past few years has revealed a number of Co-containing active sites in novel enzymes with new biological functions. The best characterized examples up to now are the Co^{III}-containing nitrile[5] or thiocyanate[6] hydrolases, the three-dimensional structures of which have been determined by X-ray crystallography, and their Co-active sites modeled by a wealth of Co^{III} coordination compounds.[7] On the other hand, the presence of Co^{II} or Zn^{II} has been documented in the active site of the enzymes ATP sulfurylase[8] and adenylate kinase.[9] In these biological systems, the Co-active site is dominated by a sulfur rich coordination sphere, either by intact or post-translationally oxidized S(Cys) thiolates.

Moreover, in addition to the native Co enzymes, during the last thirty or so years, Co-active sites have been created by substituting Co^{II} for either paramagnetic metal ions like Fe^{II}, and Cu^{II} or, even more extensively, diamagnetic ones like Zn^{II} or Cd^{II}. Representative examples of substitution by Co^{II}

*To whom correspondence should be addressed. E-mail: Kyritsis@chem.uoa.gr (P.K.), egroenen@molphys.leidenuniv.nl (E.J.J.G.).

(1) *The Biological Chemistry of the Elements*; Frausto da Silva, J. J. R., Williams, R. J. P., Eds.; Oxford University Press: Oxford, 2001.
(2) Randaccio, L.; Geremia, S.; Wuerges, J. *J. Organomet. Chem.* **2007**, *692*, 1198–1215.
(3) Pratt, D. A.; van der Donk, W. A. *Chem. Commun.* **2006**, *5*, 558–560.
(4) Randaccio, L.; Geremia, S.; Nardin, G.; Wuerges, J. *Coord. Chem. Rev.* **2006**, *250*, 1332–1350.
(5) Miyanaga, A.; Fushinobu, S.; Ito, K.; Wakagi, T. *Biochem. Biophys. Res. Commun.* **2001**, *288*, 1169–1174.
(6) Arakawa, T.; Kawano, Y.; Kataoka, S.; Katayama, Y.; Kamiya, N.; Yohda, M.; Odaka, M. *J. Mol. Biol.* **2007**, *366*, 1497–1509.
(7) Kovacs, J. A. *Chem. Rev.* **2004**, *104*, 825–848.
(8) Gavel, O. Y.; Bursakov, S. A.; Calvete, J. J.; George, G. N.; Moura, J. J. G.; Moura, I. *Biochemistry* **1998**, *37*, 16225–16232.
(9) Gavel, O. Y.; Bursako, S. A.; Di Rocco, G.; Trincao, J.; Pickering, I. J.; George, G. N.; Calvete, J. J.; Shnyrov, V. L.; Brondino, C. D.; Pereira, A. S.; Lamprela, J.; Tavares, P.; Moura, J. J. G.; Moura, I. *J. Inorg. Biochem.* **2008**, *102*, 1380–1395.

Published on Web 12/21/2009

are the Fe protein rubredoxin[10] and the blue Cu protein amicyanin,[11] with $Co^{II}[S(Cys)_4]$ and $Co^{II}[S(Sys)\text{-}S(Met)\text{-}N(His)_2]$ active sites, respectively, as revealed by X-ray crystallography. Moreover, Co^{II} has also been introduced into the active site of the ferric uptake protein (FUR),[12] the Cu-enzyme amine oxidase,[13] and the Mn-enzyme superoxide dismutase.[14] Owing to the fact that $3d^{10}$ Zn^{II} is spectroscopically silent and diamagnetic, numerous Zn-enzymes have been frequently reconstituted by Co^{II}, with the formation of S(Cys)-rich coordination spheres around Co^{II}. The main interest in such experiments stems from the fact that the $3d^7$ Co^{II}-substituted active sites are amenable to biophysical characterization by various spectroscopic (UV−vis, magnetic circular dichroism (MCD)) and magnetic methods (magnetism, paramagnetic NMR, electron paramagnetic resonance (EPR), electron−nuclear double resonance (ENDOR)). Representative examples in this case are the enzymes alcohol dehydrogenase,[15] metallo-beta-lactamase,[16,17] various aminopeptidases,[18]and phosphotriesterases,[19] as well as the Zn^{II} or Cd^{II} metallothioneins,[20] and the transcription factors known as "Zn-fingers".[21−23] The coordination of Co^{II} to S-containing ligands has also been studied by using peptides or "maquettes" as a coordination framework, aiming at retaining critical structural and spectroscopic properties of analogous Co^{II} biological sites.[24−28]

To study the catalytic function of the Co^{II}-active sites in the above-mentioned native or reconstituted enzymes, it is necessary to elucidate the electronic properties of the site. Owing to the paramagnetic nature of the Co^{II}-active sites, one of the most frequently employed spectroscopic techniques is EPR. Indeed, the EPR properties of native or reconstituted biological Co-active sites have been probed by either continuous wave (cw) [16,29] or, more recently, by pulsed EPR techniques.[23] Moreover, a wealth of Co^{II} complexes with various coordination spheres have also been studied by EPR or MCD spectroscopy, and their properties compared with those of biological Co^{II}-active sites. In that respect, most of the Co^{II} complexes studied so far contain coordination spheres dominated by either O or N atoms, whereas the presence of S-ligation is rather limited.[30−35] Studies on $Co^{II}S_4$-coordinated sites, containing various aromatic thiols as ligands and different counterions, have been reported by Hirota and co-workers, in three successive articles reporting data derived by magnetism and X-band EPR experiments.[36−38] These studies included EPR experiments on oriented single crystals, which revealed the orientation of the g-tensor's principal axes. In addition, the complexes studied were shown to exhibit large zero-field splitting (ZFS),[39] ranging between 2 and 100 cm^{-1}, whereas the rhombicity ($\lambda = E/D$) was between 0 and 0.3. On the other hand, high frequency EPR studies on Co^{2+} ions embedded in CdS have shown rather small ZFS values.[40]

The magnitude of the ZFS of Co^{II} and other paramagnetic metal complexes determined so far by various experimental methods has been reviewed in various publications.[30,31,41] Significant discrepancies in the reported data have shown that the reliable determination of the ZFS is not an easy task, and would require careful implementation of various techniques such as studies of magnetic susceptibility, EPR, VT-MCD, or Far-infrared (Far-IR) magnetic spectroscopy.[41] Thus, following the recent development in high-frequency and high-field EPR (HFEPR) methods, a reliable ZFS value has been determined for a powdered sample of $Co(PPh_3)_2Cl_2$, and its magnitude was compared to that of the same and other Co^{II} complexes derived from different experimental methods, like variable-temperature and variable-field MCD (VTVH-MCD) spectroscopy.[39] The ZFS value obtained for $Co(PPh_3)Cl_2$ from these investigations was considered as the only reference value in a recent theoretical study of the MCD spectra of a series of Co^{II} compounds.[35] Furthermore, in the

(10) Maher, M.; Cross, M.; Wilce, M. C. J.; Guss, J. M.; Wedd, A. G. *Acta Crystallogr.* **2004**, *D60*, 298–303.
(11) Carrell, C. J.; Wang, X. T.; Jones, L. M.; Jarrett, W. L.; Davidson, V. L.; Mathews, F. S. *Biochemistry* **2004**, *43*, 9381–9389.
(12) Adrait, A.; Jacquamet, L.; Le Pape, L.; de Peredo, A. G.; Aberdam, D.; Hazemann, J. L.; Latour, J. M.; Michaud-Soret, I. *Biochemistry* **1999**, *38*, 6248–6260.
(13) Mills, S. A.; Goto, Y.; Su, Q. J.; Plastino, J.; Klinman, J. P. *Biochemistry* **2002**, *41*, 10577–10584.
(14) Whittaker, M. M.; Mizuno, K.; Bachinger, H. P.; Whittaker, J. W. *Biophys. J.* **2006**, *90*, 598–607.
(15) Werth, M. T.; Tang, S. F.; Formicka, G.; Zeppezauer, M.; Johnson, M. K. *Inorg. Chem.* **1995**, *34*, 218–228.
(16) Periyannan, G. R.; Costello, A. L.; Tierney, D. L.; Yang, K. W.; Bennett, B.; Crowder, M. W. *Biochemistry* **2006**, *45*, 1313–1320.
(17) Tioni, M. F.; Llarrull, L. I.; Poeylaut-Palena, A. A.; Marti, M. A.; Saggu, M.; Periyannan, G. R.; Mata, E. G.; Bennett, B.; Murgida, D. H.; Vila, A. J. *J. Am. Chem. Soc.* **2008**, *130*, 15852–15863.
(18) Munih, P.; Moulin, A.; Stamper, C. C.; Bennett, B.; Ringe, D.; Petsko, G. A.; Holz, R. C. *J. Inorg. Biochem.* **2007**, *101*, 1099–1107.
(19) Rochu, D.; Beaufet, N.; Renault, F.; Viguie, N.; Masson, P. *Biochim. Biophys. Acta* **2002**, *1594*, 207–218.
(20) Peroza, E. A.; Freisinger, E. *J. Biol. Inorg. Chem.* **2007**, *12*, 377–391.
(21) Ghering, A. B.; Shokes, J. E.; Scott, R. A.; Omichinski, J. G.; Godwin, H. A. *Biochemistry* **2004**, *43*, 8346–8355.
(22) Guerrerio, A. L.; Berg, J. M. *Biochemistry* **2004**, *43*, 5437–5444.
(23) Walsby, C. J.; Krepkiy, D.; Petering, D. H.; Hoffman, B. M. *J. Am. Chem. Soc.* **2003**, *125*, 7502–7503.
(24) Anglin, J. R.; Davison, A. *Inorg. Chem.* **1975**, *14*, 234–237.
(25) Lombardi, A.; Marasco, D.; Maglio, O.; Di Costanzo, L.; Nasti, F.; Pavone, V. *Proc. Nat. Acad. Sci., U.S.A.* **2000**, *97*, 11922–11927.
(26) Nivorozhkin, A. L.; Segal, B. M.; Musgrave, K. B.; Kates, S. A.; Hedman, B.; Hodgson, K. O.; Holm, R. H. *Inorg. Chem.* **2000**, *39*, 2306–2313.
(27) Petros, A. K.; Shaner, S. E.; Costello, A. L.; Tierney, D. L.; Gibney, B. R. *Inorg. Chem.* **2004**, *43*, 4793–4795.
(28) Nanda, V.; Rosenblatt, M. M.; Osyczka, A.; Kono, H.; Getahun, Z.; Dutton, P. L.; Saven, J. G.; DeGrado, W. F. *J. Am. Chem. Soc.* **2005**, *127*, 5804–5805.
(29) Kuo, L. C.; Makinen, M. W. *J. Am. Chem. Soc.* **1985**, *107*, 5255–5261.
(30) Makinen, M. W.; Kuo, L. C.; Yim, M. B.; Wells, G. B.; Fukuyama, J. M.; Kim, J. E. *J. Am. Chem. Soc.* **1985**, *107*, 5245–5255.
(31) Larrabee, J. A.; Alessi, C. M.; Asiedu, E. T.; Cook, J. O.; Hoerning, K. R.; Klingler, L. J.; Okin, G. S.; Santee, S. G.; Volkert, T. L. *J. Am. Chem. Soc.* **1997**, *119*, 4182–4196.
(32) Johansson, F. B.; Bond, A. D.; Nielsen, U. G.; Moubaraki, B.; Murray, K. S.; Berry, K. J.; Larrabee, J. A.; McKenzie, C. J. *Inorg. Chem.* **2008**, *47*, 5079–5092.
(33) Larrabee, J. A.; Chyun, S. A.; Volwiler, A. S. *Inorg. Chem.* **2008**, *47*, 10499–10508.
(34) Rosa, V.; Gonzales, P. J.; Avilés, T.; Gomes, P. T.; Welter, R.; Rizzi, A. C.; Passeggi, M. C. G.; Brondino, C. D. *Eur. J. Inorg. Chem.* **2006**, *2006*, 4761–4769.
(35) Sundararajan, M.; Ganyushin, D.; Ye, S.; Neese, F. *Dalton Trans.* **2009** 10.1039/b902743b.
(36) Fukui, K.; Ohyanishiguchi, H.; Hirota, N. *Bull. Chem. Soc. Jpn.* **1991**, *64*, 1205–1212.
(37) Fukui, K.; Kojima, N.; Ohyanishiguchi, H.; Hirota, N. *Inorg. Chem.* **1992**, *31*, 1338–1344.
(38) Fukui, K.; Masuda, H.; Ohyanishiguchi, H.; Kamada, H. *Inorg. Chim. Acta* **1995**, *238*, 73–81.
(39) Krzystek, J.; Zvyagin, S. A.; Ozarowski, A.; Fiedler, A. T.; Brunold, T. C.; Telser, J. *J. Am. Chem. Soc.* **2004**, *126*, 2148–2155.
(40) Bindilatti, V.; Anisimov, A. N.; Oliveira, N. F.; Shapira, Y.; Goiran, M.; Yang, F.; Isber, S.; Averous, M.; Demianiuk, M. *Phys. Rev. B* **1994**, *50*, 16464–16467.
(41) Boca, R. *Coord. Chem. Rev.* **2004**, *248*, 757–815.

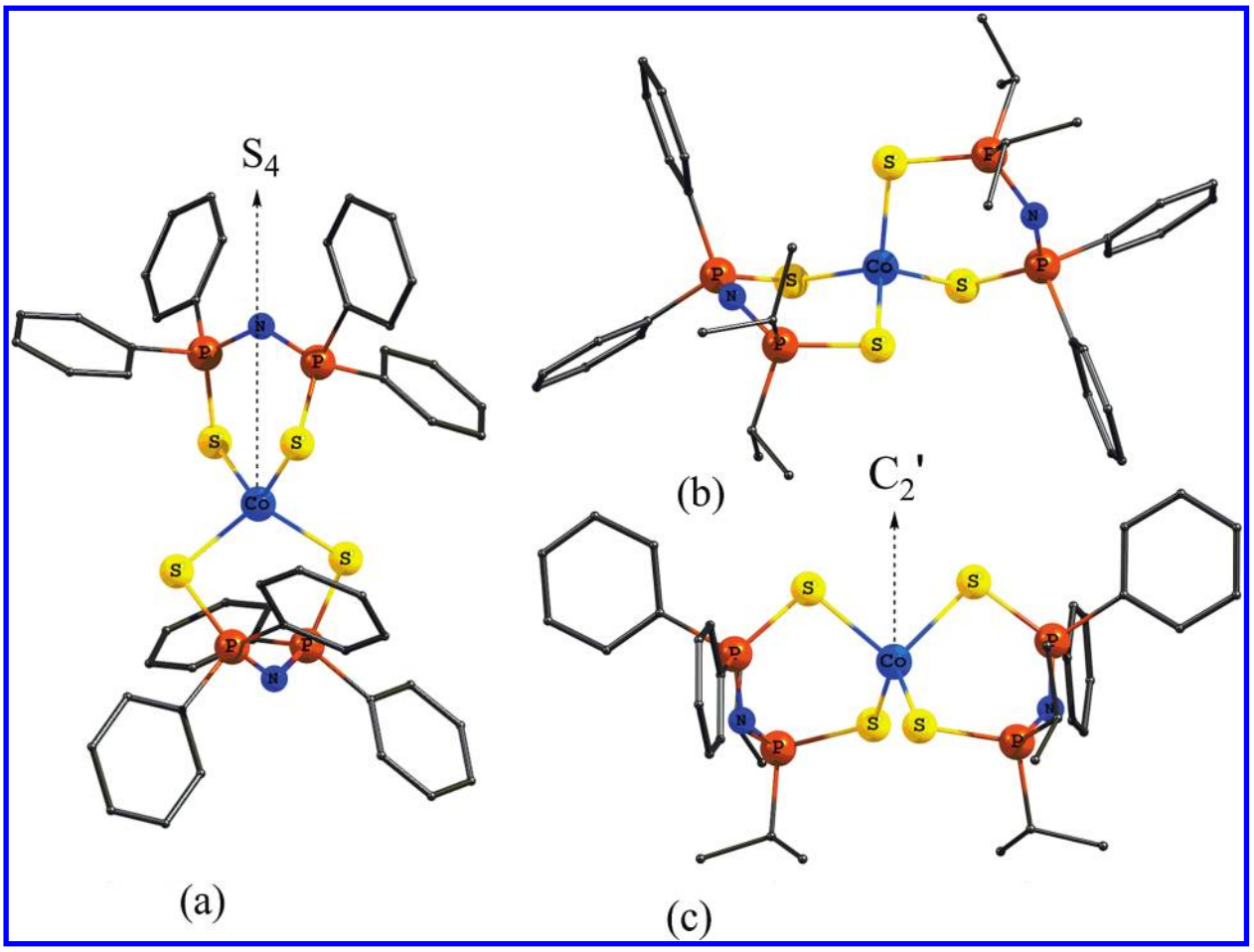

Figure 1. Molecular structures of (a) $Co^{Ph,Ph}L_2$ and (b, c) $Co^{iPr,Ph}L_2$. In (a) and (c) the (approximate) symmetry axes are indicated, while the view in (b) is such that the symmetry axis is perpendicular to the plane of the paper.

EPR spectra obtained so far on Co(II) systems, the cobalt hyperfine interaction is commonly not resolved.

The above considerations show that it is of prime importance to extend the data set of EPR properties on Co^{II} coordination compounds, including more examples of $Co^{II}S_4$ coordination, in an attempt to correlate their electronic properties, derived by EPR experiments, with their structural properties. To that direction, an appropriate choice was a series of $Co^{II}S_4$-containing CoL_2 complexes, obtained by employing the bidentate disulfidoimidodiphosphinato ligands LH of the type $R_2P(S)NHP(S)R'_2$, R, R′ = Ph or ^{i}Pr.[42−44] The first $Co^{II}S_4$-containing complex bearing such ligands, $Co[(SPPh_2)_2N]_2$, which will be denoted as $Co^{Ph,Ph}L_2$, was reported in 1971,[45] and its crystallographic structure, along with the structure of the analogous complex containing R = ^{i}Pr, $Co[(SP^{i}Pr_2)_2N]_2$, was determined more recently.[46] In addition to the CoL_2 complexes bearing symmetric disulfidoimidodiphosphinato ligands, the corresponding complex containing R = Ph and R′ = ^{i}Pr, $Co[(SPPh_2)(SP^{i}Pr_2)N]_2$, denoted as $Co^{iPr,Ph}L_2$, has recently been synthesized and structurally characterized.[47] The spectroscopic and magnetic properties of the above-mentioned $Co^{II}S_4$-containing complexes were investigated in combination with theoretical calculations, with the focus on the covalency of their Co^{II}−S bonds.[47] These complexes present the advantages of (i) being stable with respect to oxidation of the metal ion, (ii) providing the possibility to alter their "second coordination sphere" by employing different peripheral R groups on the ligand, which would affect the structural and electronic properties of the metal site, and (iii) showing $Co^{II}S_4$-coordination spheres with different degrees of distortion from the ideal tetrahedral geometry because the $Co^{Ph,Ph}L_2$ and $Co^{iPr,Ph}L_2$ complexes possess S_4 and C_2' symmetry (Figure 1), respectively, the consequences of which would be very interesting to probe by EPR.

Here we report the results of extensive EPR studies on the $Co^{Ph,Ph}L_2$ and $Co^{iPr,Ph}L_2$ complexes, in which various types of samples (microcrystalline powders, single crystals, magnetically diluted crystals to the analogous ZnL_2 complexes) and various microwave frequencies and magnetic fields have been employed. Accurate values of the ZFS, the effective g tensor and the cobalt hyperfine interaction tensor were determined. The EPR observables show that the structural differences between the two complexes, imposed by the

(42) Ly, T. Q.; Woollins, J. D. *Coord. Chem. Rev.* **1998**, *176*, 451–481.
(43) Silvestru, C.; Drake, J. E. *Coord. Chem. Rev.* **2001**, *223*, 117–216.
(44) Haiduc, I. Dichalcogenoimidodiphosphinato Ligands. In Comprehensive Coordination Chemistry II: From Biology to Nanotechnology, Eds. McCleverty, J. A., Meyer, T. J. In *Fundamentals*; Lever, A. B. P., Ed., Elsevier: Amsterdam, 2004; Vol. *1*, pp 323−347;
(45) Davison, A.; Switkes, E. S. *Inorg. Chem.* **1971**, *10*, 837–842.
(46) Gilby, L. M.; Piggott, B. *Polyhedron* **1999**, *18*, 1077–1082.
(47) Maganas, D.; Staniland, S. S.; Grigoropoulos, A.; White, F.; Parsons, S.; Robertson, N.; Kyritsis, P.; Pneumatikakis, G. *Dalton Trans.* **2006**, *19*, 2301–2315.

nature of the peripheral R groups (R = Ph or ^{i}Pr) in the "second coordination sphere", affect significantly the electronic structure of the $Co^{II}S_4$ core.

Experimental Section

Synthesis of Co^{II} Complexes. All experiments were carried out under an atmosphere of argon using Schlenk techniques. Glassware was dried in the oven at approximately 110 °C and baked out in vacuo prior to use. The solvents were dried by standard methods (methanol and dichloromethane over CaH_2, *n*-hexane over sodium wire) and distilled under argon. The solvents were deoxygenated by at least two freeze−pump−thaw cycles immediately prior to use. Electronic spectra were recorded in a Cary 300 Varian spectrophotometer. $^{31}P\{^{1}H\}$ NMR spectra were recorded in a Varian Unity Plus 300 MHz instrument, and the reported chemical shifts are relative to 85% H_3PO_4.

The synthesis of $Co^{Ph,Ph}L_2$ and $Co^{iPr,Ph}L_2$ was carried out according to published procedures.[46,47] To optimize the sensitivity of the EPR measurements, specific samples were considered. For that purpose, fine powder samples, single crystals, and magnetically diluted crystals to the analogous ZnL_2 complexes of $Co^{Ph,Ph}L_2$ and $Co^{iPr,Ph}L_2$ were prepared.

For the preparation of fine powder samples, an appropriate amount of powdered $Co^{Ph,Ph}L_2$ (∼10 mmol) was dissolved in the minimum amount of dichloromethane (∼10 mL). Subsequently, *n*-hexane (1:4) was added rapidly under continuous stirring. Immediately, microcrystals of such small size they can be defined as fine powder, were formed. The precipitate was subsequently collected by filtration. The $Co^{iPr,Ph}L_2$ complex was isolated as a fine powder.[47]

Single crystals of $Co^{Ph,Ph}L_2$ and $Co^{iPr,Ph}L_2$ were obtained by slowly mixing a dichloromethane solution of each complex with *n*-hexane and methanol, respectively, in 1:3 ratio. This procedure resulted in dark green and dark blue needle-like crystals, respectively.

The synthesis of $Zn^{Ph,Ph}L_2$ was first reported in 1971 but its crystallographic characterization has been recently accomplished.[48] The synthesis of $Zn^{iPr,Ph}L_2$ was carried out according to published procedures.[49]

Magnetic dilution methods were employed to diminish the dipolar interactions between the paramagnetic Co^{II} (S = 3/2) centers such that the hyperfine interaction between the electron spin and the cobalt nuclear spin (I = 7/2) could be resolved in the EPR spectrum. The $Co^{Ph,Ph}L_2$ and $Co^{iPr,Ph}L_2$ complexes were cocrystallized into the diamagnetic host crystal matrix of their respective Zn^{II} analogues, $Zn^{Ph,Ph}L_2$ and $Zn^{iPr,Ph}L_2$, to form 1% Co^{II}/Zn^{II}-doped single cocrystals. The UV−vis spectra of solutions of 5% and 50% $Co^{Ph,Ph}L_2/Zn^{Ph,Ph}L_2$ cocrystals dissolved in CH_2Cl_2 are shown in Figure S1, along with the $^{31}P\{^{1}H\}$ NMR spectrum of the 50% cocrystallized system. Such spectra enable an estimate as to the degree of magnetic dilution of crystals, which was found to be larger than in the solutions from which the crystals were grown.

EPR Experiments. The measurements at X- and W-band frequencies were performed on a Bruker Elexsys E680 spectrometer. The X-band spectra were obtained using 100 kHz field modulation, with an amplitude of 0.5−1.5 mT, depending on the line width. The W-band spectra were obtained at a modulation frequency of 80 kHz, with an amplitude of 1 mT.

The X-band spectra of polycrystalline powders of $Co^{Ph,Ph}L_2$ and $Co^{iPr,Ph}L_2$ were recorded with the sample in the superconducting magnet, belonging to the W-band part of the spectrometer, in combination with the X-band bridge for microwave generation and detection. In this way, X-band spectra have been acquired up to fields of 3 T. Use was made of the dielectric resonator (Flexline, frequency about 9.7 GHz). The probe-head support was modified to position the resonator active volume in the center of the magnet homogeneity zone and to fit into the cryostat of the W-band probe-head.

The single-crystal measurements at X-band were carried out in the electromagnet using the rectangular TE_{102} cavity, equipped with the ESR 900 Cryostat (Oxford Instruments). To enable sample rotation about two orthogonal axes, a new sample holder was constructed compatible with the ESR 900 cryostat and operating from room temperature to about 4 K. This device has been described elsewhere.[50]

For temperature-dependent measurements, the calibration of the temperature was performed as follows: a Lake Shore Carbon-Glass sensor (CGR-1 series) was calibrated in a commercial Quantum Design physical properties measurement system (PPMS) and subsequently placed at the sample position in the cryostat. The Oxford temperature unit was then calibrated against this sensor.

The J-band (275 GHz) spectrum of polycrystalline powder of $Co^{iPr,Ph}L_2$ was measured on a home-built spectrometer,[51] using 1.2 kHz field modulation of about 0.2 mT amplitude. To avoid self-orientation of the microcrystals in the high magnetic field (up to 12 T), the powder was pressed into the sample tube using a tiny amount of cotton.

Theory

The description of the EPR spectra of the high-spin Co^{II} complexes (S = 3/2) is based upon the spin Hamiltonian that includes the ZFS, the electron Zeeman interaction, and the cobalt hyperfine and nuclear Zeeman interaction.

$$H_S = \vec{S}\,.\,\vec{\vec{D}}\,.\vec{S} + \mu_B \vec{S}\,.\,\vec{\vec{g}}\,.\vec{B} + \vec{S}\,.\,\vec{\vec{A}}\,.\vec{I} - g(Co)\mu_N \vec{I}\,.\vec{B} \quad (1)$$

where $\vec{S}$ and $\vec{I}$ represent the electron-spin and cobalt nuclear-spin angular momentum operators and the $\vec{\vec{D}}$, $\vec{\vec{g}}$ and $\vec{\vec{A}}$ tensors represent the interactions. A full description of the S = 3/2 case can be found in textbooks.[52] Here we introduce part of the theoretical results and present the equations as used in the analysis of the EPR data of the cobalt complexes. Note that the low symmetry of the cobalt complexes under study precludes us from assuming the principal axes of $\vec{\vec{D}}$ and $\vec{\vec{g}}$ being parallel.

The first term in eq 1 gives rise to four magnetic sublevels, which form two Kramers doublets,

$$\cos\theta\left|\frac{3}{2}, \pm\frac{3}{2}\right\rangle + \sin\theta\left|\frac{3}{2}, \mp\frac{1}{2}\right\rangle$$

$$\cos\theta\left|\frac{3}{2}, \pm\frac{1}{2}\right\rangle - \sin\theta\left|\frac{3}{2}, \mp\frac{3}{2}\right\rangle \quad (2)$$

where the angle θ in terms of the ZFS parameters is given by $tg2\theta = \sqrt{3}E/D \equiv \sqrt{3}\lambda$. The energy separation between the doublets amounts to 2D′, with D′ given by

(48) Maganas, D.; Raptopoulou, C. P.; Psycharis, V.; Kyritsis, P. unpublished results.

(49) Birdsall, D. J.; Slawin, A. M. Z.; Woollins, J. D. *Polyhedron* **2001**, *20*, 125–134.

(50) Milikisyants, S.; Sottini, S.; Disselhorst, J.; van der Meer, H.; Groenen, E. J. J. *Rev. Sci. Instrum.* **2008**, *79*(4), article number 046107.

(51) Blok, H.; Disselhorst, J. A. J. M.; Orlinski, S. B.; Schmidt, J. *J. Magn. Reson.* **2004**, *166*, 92–99.

(52) *Principles of Electron Spin Resonance*; Atherton, N. M., Ed; Ellis Horwood PTR Prentice Hall, 1993.

$\left(D^2+3E^2\right)^{1/2}$. The ZFS parameters are defined in terms of the principal values of the $\vec{\vec{D}}$ tensor by $D \equiv \frac{3}{2}D_z$ and $E \equiv \frac{1}{2}(D_x - D_y)$. Although m_s is not a good quantum number, we will refer to the doublets as $\pm 3/2$ and $\pm 1/2$, respectively.

In a small magnetic field, such that the electron Zeeman interaction is much smaller than the zero-field interaction, the effect of the second term in eq 1 on the energy of the levels may be obtained by considering the doublets separately. Both for the $\pm 1/2$ and the $\pm 3/2$ doublet, the energies may be written in the effective $S = 1/2$ picture as

$$E = \pm \frac{1}{2}\mu_B B\left\{\sum_\beta \left(\sum_\alpha \ell_\alpha g'_{\alpha\beta}\right)^2\right\}^{1/2} \tag{3}$$

Here α,β = x,y,z and $\vec{l}$ represents a unit vector in the direction of $\vec{B}$ in the reference axes system x,y,z.

$$\text{The effective g'matrix is defined by } g'_{\alpha\beta} = g_{\alpha\beta}\omega_\beta \tag{4}$$

with

$$\begin{aligned}\omega_x &= \left(2\sqrt{3}\cos\theta\sin\theta + 2\sin^2\theta\right)\\ \omega_y &= \left(2\sqrt{3}\cos\theta\sin\theta - 2\sin^2\theta\right)\\ \omega_z &= \left(3\cos^2\theta - \sin^2\theta\right)\end{aligned} \tag{5}$$

for the $\pm 3/2$ doublet. The corresponding expressions for the $\pm 1/2$ doublet are obtained by replacing $\cos\theta$ by $-\sin\theta$ and $\sin\theta$ by $\cos\theta$.

In the particular case that the principal axes of $\vec{\vec{D}}$ and $\vec{\vec{g}}$ coincide, eq 4 turns into the well-known relations between the principal values of g′ and g in terms of the parameter λ.[53]

For larger magnetic fields, when the low-field approximation no longer applies, the eigenvalues corresponding to the first two terms of the spin Hamiltonian in eq 1 are no longer proportional to B. For coincidence of the principal axes of $\vec{\vec{D}}$ and $\vec{\vec{g}}$, analytical expressions have been obtained for orientations of $\vec{B}$ parallel to the principal axes.[52] For $\vec{B}$ //z, the energy of the magnetic sublevels may be written as

$$E = \pm\frac{1}{2}\mu_B B g_z - \left[\left\{D_z - \frac{1}{2}(D_x + D_y) \pm \mu_B B g_z\right\}^2 + \frac{3}{4}(D_x - D_y)^2\right]^{1/2} \tag{6}$$

$$E = \pm\frac{1}{2}\mu_B B g_z + \left[\left\{D_z - \frac{1}{2}(D_x + D_y) \pm \mu_B B g_z\right\}^2 + \frac{3}{4}(D_x - D_y)^2\right]^{1/2} \tag{7}$$

where for negative D the energies in eq 6 refer to the $\pm 1/2$ doublet and in eq 7 refer to the $\pm 3/2$ doublet. For positive D the reverse applies. Cyclic permutation of x, y, and z yields the corresponding expressions for $\vec{B}$ //x and $\vec{B}$ //y. In these expressions g_x, g_y, and g_z refer to the principal values of the g matrix.

The cobalt nuclear spin $I = 7/2$ may result in a splitting of the lines in the EPR spectra. In case the mixing of the electron-spin states is negligible, the nuclear part of the spin Hamiltonian in eq 1 may be written as

$$H_n = \langle\vec{S}\rangle.\vec{\vec{A}}.\vec{I} - g(Co)\mu_N\vec{I}.\vec{B} \tag{8}$$

where $\langle\vec{S}\rangle$ represents the expectation value of the electron-spin angular momentum. From this Hamiltonian we find for the energy shift ΔE of the nuclear spin sublevel with quantum number m_I in the effective $S = 1/2$ picture

$$\Delta E(m_I) = m_I\left\{\sum_\delta \left(\sum_\gamma \langle S_\gamma\rangle A_{\gamma\delta} - g_{Co}\mu_N B\ell_\delta\right)^2\right\}^{1/2} \tag{9}$$

where γ,δ = x′,y′,z′ and x′,y′,z′ represents the principal axes system of the g′ tensor.

The expectation values for the two substates of the doublet are given by

$$\langle S_\gamma\rangle = \pm\frac{1}{2}\omega_\gamma\ell_\gamma g'_\gamma/g' \tag{10}$$

where g'_γ represents the principal values of the g′ matrix and

$$g' = \left\{\sum_\gamma \ell_\gamma^2\, g'^2_\gamma\right\}^{1/2} \tag{11}$$

In terms of the effective hyperfine tensor A′ defined by

$$A'_{\gamma\delta} = \omega_\gamma A_{\gamma\delta} \tag{12}$$

eq 9 becomes

$$\Delta E^{\pm}(m_I) = m_I\left\{\sum_\delta \left(\pm\frac{1}{2}\sum_\gamma \ell_\gamma g'_\gamma A'_{\gamma\delta}/g' - g_{Co}\mu_N B\ell_\delta\right)^2\right\}^{1/2} \tag{13}$$

At temperatures such that $kT \ll ZFS$, only the lowest doublet (1) will be occupied. Upon temperature increase, the higher doublet (2) becomes populated as well, and the EPR transition within this doublet may become detectable. Its intensity will be proportional to the population difference between the sublevels of doublet (2) given by

$$e^{-2D'/kT}/\left[T\left(1 + e^{-2D'/kT}\right)\right] \tag{14}$$

The ratio of the intensities of the transitions in both doublets becomes

$$\frac{I_1}{I_2} = \frac{P_1}{P_2}e^{2D'/kT} \tag{15}$$

(53) Banci, L.; Bencini, A.; Benelli, C.; Gatteschi, D.; Zanchini, C. *Struct. Bonding* (*Berlin*) **1982**, *12*, 37–86.

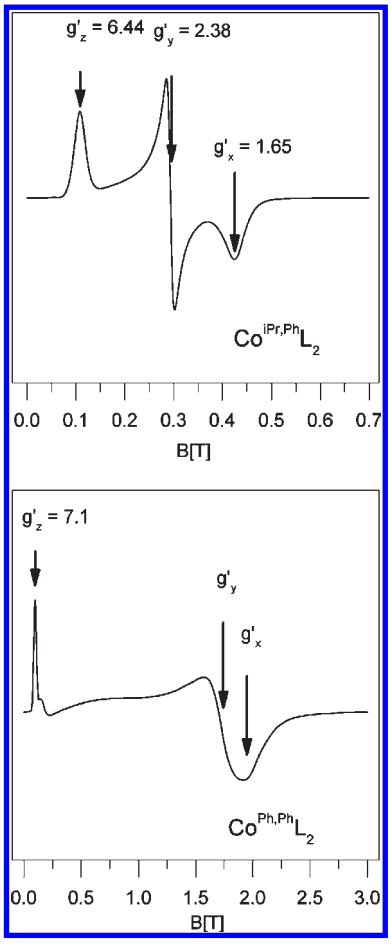

Figure 2. EPR spectra of powder samples of $Co^{Ph,Ph}L_2$ and $Co^{iPr,Ph}L_2$ at X-band and 8K.

where P_1 and P_2 refer to the probabilities of the transitions within the respective doublets. For not too large magnetic fields, the zero-field functions (eq 2) may be used and the ratio of the transition probabilities may be written in terms of θ. In case the $\pm 3/2$ doublet is lowest in energy

$$\frac{P_1}{P_2} = \left\{ \frac{\sqrt{3}\mathrm{tg}\theta + \mathrm{tg}^2\theta}{1 - \sqrt{3}\mathrm{tg}\theta} \right\}^2 \qquad (16)$$

Results

Figure 2 shows the cw X-band EPR spectra of powder samples of $Co^{Ph,Ph}L_2$ and $Co^{iPr,Ph}L_2$ in a superconducting magnet at about 8 K. A pronounced difference is observed between the two complexes. The g′ values reveal that the effective g-tensor is rhombic for $Co^{iPr,Ph}L_2$, whereas it is nearly axial for $Co^{Ph,Ph}L_2$. The EPR spectra are determined by the ZFS, the electron Zeeman interaction, and the (unresolved) cobalt hyperfine and nuclear Zeeman interaction. To unravel these respective contributions, we made use of single crystals, performed experiments at different microwave frequencies and temperatures, and studied samples of $Co^{Ph,Ph}L_2$ and $Co^{iPr,Ph}L_2$ diluted into the corresponding diamagnetic zinc complexes $Zn^{Ph,Ph}L_2$ and $Zn^{iPr,Ph}L_2$.

Zero-Field Splitting. For $Co^{Ph,Ph}L_2$, we derived the ZFS from the variation of the cw X-band EPR spectrum with temperature between 4 and 60 K. A single crystal has been studied oriented with its z′ axis (the principal z axis of the g′ tensor) about 10° away from the direction of the magnetic field $\vec{B}$. Spectra at three temperatures are represented in Figure 3a. At 5 K the spectrum shows only one relatively narrow band (called 1) at about 0.1 T. Upon increasing the temperature, the intensity of this band decreases and a broad band (called 2) arises around 0.3 T, which above 30 K quickly loses intensity as well. Band 2 corresponds to a transition within the doublet at highest energy, which becomes populated at higher temperatures. From the variation of the double integral of band 2 as a function of temperature (Figure 3b) we calculate, according to eq 14, a value of 11.9 cm^{-1} for D′. Subsequently, from the ratio of the intensity of both bands (Figure 3c), we determine P_1/P_2 according to eq 15. In doing so, we take into account the intensity ratios up to 22 K, because the error in this ratio becomes too big at higher temperatures. We find $P_1/P_2 \approx 6.10^{-3}$. The fact that the probability of transition 1 is much smaller than that of transition 2 means that the transition at lower field corresponds to the "forbidden" transition within the $\pm 3/2$ doublet, i.e., D is negative. From eq 16 we then obtain $\lambda \approx -0.05$, where the negative sign corresponds to the fact that we label the midfield transition by y.

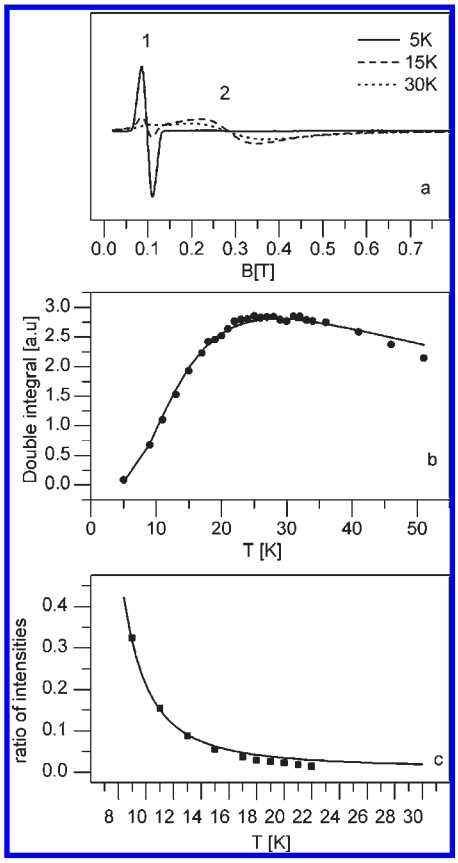

Figure 3. Temperature dependence of the X-band EPR spectrum of a single crystal of $Co^{Ph,Ph}L_2$ for an orientation of the crystal such that the external magnetic field makes an angle of about 10° with the principal z′ axis of the effective g tensor. (a) Spectra for three representative temperatures. (b) Variation of the double integral of the high-field transition (band 2) as a function of temperature. (c) Ratio of the intensities of the low- (band 1) and high-field (band 2) transition as a function of temperature.

For $Co^{iPr,Ph}L_2$, the magnitude of the ZFS was estimated from cw EPR experiments at W-band and J-band microwave frequencies. If the electron-Zeeman splitting

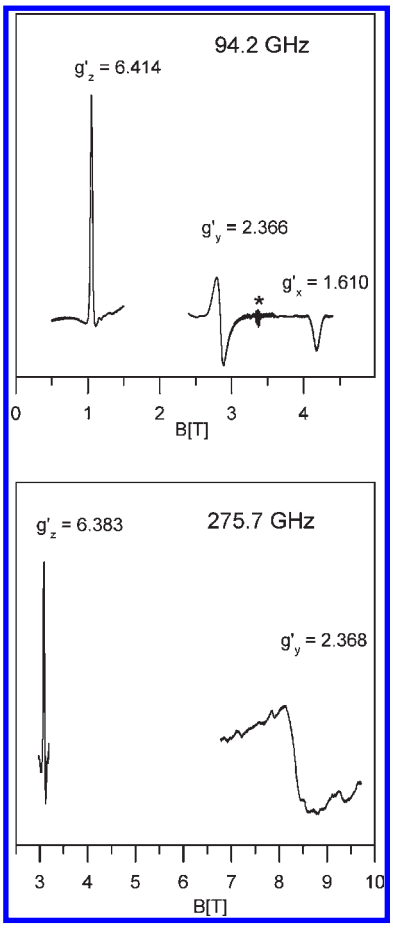

Figure 4. EPR spectra of powder samples of $Co^{iPr,Ph}L_2$ at W-band (20 K) and at J-band (6 K).

is no longer much smaller than the ZFS, deviations from the effective spin S = 1/2 description become noticeable and the g′ values become frequency dependent. Spectra of a powder sample of $Co^{iPr,Ph}L_2$ at 94.2 and 275.7 GHz are shown in Figure 4. The spectrum at 94.2 GHz shows the same effective g'_y value, within experimental error, as for X-band (cf. Figure 2a), but a clear decrease of g'_x. At 275.7 GHz we can only detect the z and y transitions. The g'_y value is still about the same, but the g'_z value is now clearly smaller than at lower microwave frequencies. From the fields of resonance in W- and J-band we obtain, according to eq 7: $|D| = 12.9\ cm^{-1}$ and $\lambda = -0.33$, corresponding to a value of about $14.8\ cm^{-1}$ for D′. Note that the labeling of the transitions corresponds to the interpretation in which the EPR spectra derive from the ±3/2 doublet. In case the EPR spectra derive from the ±1/2 doublet, the x and z labels should be interchanged but the estimated value of the ZFS remains the same. This result relates to the fact that $\lambda = |1/3|$ (see Discussion).

Effective g-Tensor. To determine the complete effective g-tensor for $Co^{iPr,Ph}L_2$, including the directions of the principal axes, we have studied the X-band cw EPR spectrum at 5 K of a 1% $Co^{iPr,Ph}L_2$/ $Zn^{iPr,Ph}L_2$ single crystal as a function of the orientation of the magnetic field $\vec{B}$ with respect to the crystal.

In Figure 5, spectra are summarized for four orientations. The fields of resonance span about the full range of magnetic fields corresponding to the powder spectrum in Figure 2a. In the 1% $Co^{iPr,Ph}L_2/Zn^{iPr,Ph}L_2$ crystal, the

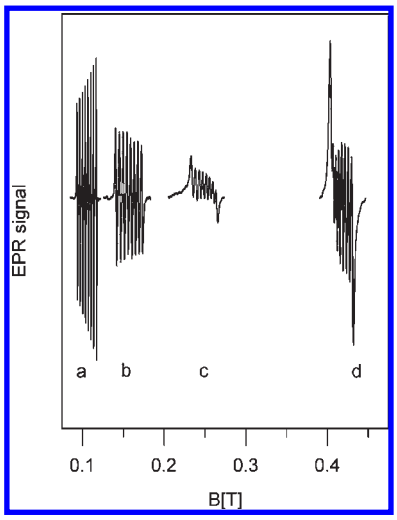

Figure 5. EPR spectra of a single crystal of 1% $Co^{iPr,Ph}L_2/Zn^{iPr,Ph}L_2$ for four orientations of the magnetic field with respect to the crystal: (a) parallel to the z′ axis, (b) 53 degrees from z′ in the y′z′ plane, (c) 77 degrees from z′ in the y′z′ plane, (d) parallel to the x′ axis. Spectra a, b, and c were obtained with the same microwave power.

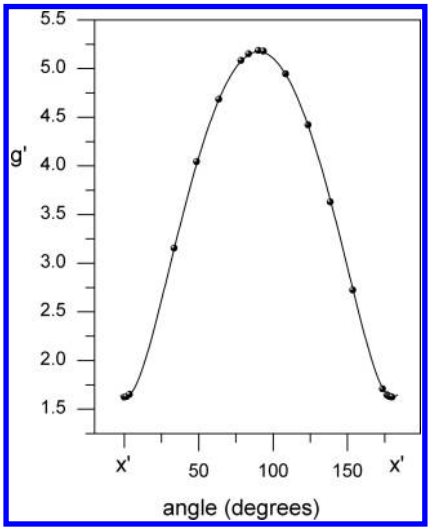

Figure 6. Variation of g′ for a single crystal of 1% $Co^{iPr,Ph}L_2/Zn^{iPr,Ph}L_2$ as a function of the orientation of the magnetic field in a plane that contains the principal x′ axis (direction corresponds to 0 degrees). The dots represent the experimental observations and the line represents the fit according to eq 3.

cobalt−cobalt dipolar interaction decreases to such an extent that the cobalt (I = 7/2) hyperfine interaction becomes fully resolved. Taking into account the fields of resonance for many orientations of $\vec{B}$ in three planes, the $(g' \cdot g')$ matrix was obtained and diagonalized. The quality of the data and the analysis is illustrated for orientations of $\vec{B}$ in one plane in Figure 6. The resulting principal g′ values are presented in Table 1. The orientation of the principal axes of the g′ tensor is obtained in a laboratory fixed axes system. Combination with an X-ray diffraction study of the crystal as mounted for the EPR measurements, enabled the translation of these directions into the crystallographic a,b,c axes system. The orientation of the principal g′ axes in the crystallographic unit cell is given in Table 1.

For $Co^{Ph,Ph}L_2$, determination of the effective g-tensor is more complicated than for $Co^{iPr,Ph}L_2$. The spectrum at X-band in Figure 2b shows that g'_y and g'_x are close to

Table 1. Effective g Tensor and the Effective Cobalt Hyperfine Tensor for $Co^{iPr,Ph}L_2$ [a]

	$g'_x = 1.62$	$g'_y = 2.38$	$g'_z = 6.44$		$\|A'_x\| = 83$	$\|A'_y\| = 50$	$\|A'_z\| = 302$
	x′	y′	z′		x″	y″	z″
a	0.447	0.003	−0.895	x′	−0.999	0	−0.027
b	0.018	0.999	0.012	y′	0	1	0
c(axb)	0.894	−0.022	0.446	z′	−0.027	0	0.999

[a] The principal hyperfine values are given in MHz. The orientation of the principal axes x′,y′,z′ of the effective g tensor is represented by their direction cosines in the crystallographic axes system a,b,c. The orientation of the principal axes x″,y″,z″ of the A′ tensor is represented by their direction cosines in the axes system x′,y′,z′.

Table 2. Effective g Tensor for $Co^{Ph,Ph}L_2$ [a]

			z′
g'_x	0.3	a	0.978
g'_y	0.3	b	−0.230
g'_z	7.12	c	−0.242

[a] The principal values and the orientation of the principal z′ axis represented by its direction cosines in the crystallographic axes system a, b,c.

zero, which means that for most orientations of $\vec{B}$ with respect to a single crystal, the contribution of g'_y and g'_x to the effective g′ value is negligible. In addition, the value of E is about zero in this case, which corresponds to a low intensity of the ±3/2 transition. Consequently, the transitions in the plane perpendicular to the principal z′ axis were only observed for a few orientations of the magnetic field.

We have studied the X-band cw EPR spectrum at 5 K of a 1% $Co^{Ph,Ph}L_2/Zn^{Ph,Ph}L_2$ single crystal, as a function of the orientation of $\vec{B}$ with respect to the crystal, in a way similar to the investigation for $Co^{iPr,Ph}L_2$. From the fields of resonance for many orientations of $\vec{B}$ in three planes we obtained the principal g′ values. In addition, we obtained the direction of the principal z′ axis in a laboratory fixed coordinate system and, from a combination with X-ray diffraction data, in the crystallographic axes system. Both the g′ values and the orientation of the z′ axis are given in Table 2.

Cobalt Hyperfine Interaction. The cobalt hyperfine interaction does not result in resolved hyperfine structure for solution (for examples see Figure S2), powder (Figures 2 and 4) or crystalline (Figure 3) samples, neither for $Co^{Ph,Ph}L_2$ nor for $Co^{iPr,Ph}L_2$. For diluted powders of CoL_2 in the diamagnetic ZnL_2, cobalt hyperfine structure gets resolved in the low-field transition corresponding to g'_z. Upon dilution of the CoL_2 complex in the host crystal of the corresponding diamagnetic ZnL_2 complex, hyperfine splitting may show up at all fields as shown for a 1% $Co^{iPr,Ph}L_2/Zn^{iPr,Ph}L_2$ single crystal in Figure 5. As long as the mixing of electron-spin states by the hyperfine interaction is negligible, eq 9 applies, which points to eight equidistant lines. This comes close to the experimental observations, but slight systematic deviations are observed. This is illustrated in Figure 7, for the orientation of $\vec{B}$ parallel to the principal z′ axis. The hyperfine splitting increases with increasing magnetic field, the separation between the two highest-field components being about 1% larger than that between the two lowest-field components. The separation between the $m_I = \pm n/2$ lines (n = 3,5,7) lines is found to be n times the separation between the inner $m_I = \pm 1/2$ lines, which

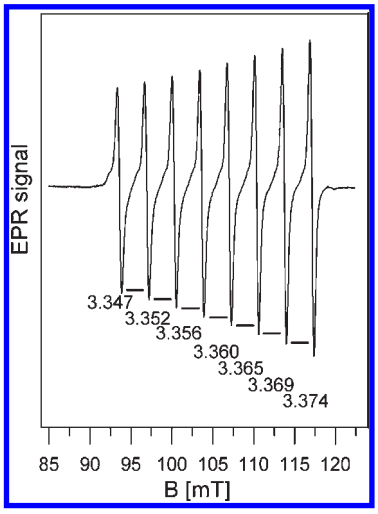

Figure 7. EPR spectrum of a single crystal of 1% $Co^{iPr,Ph}L_2/Zn^{iPr,Ph}L_2$ for the magnetic field parallel to the principal z′ axis. The cobalt hyperfine splitting gradually increases at higher magnetic fields.

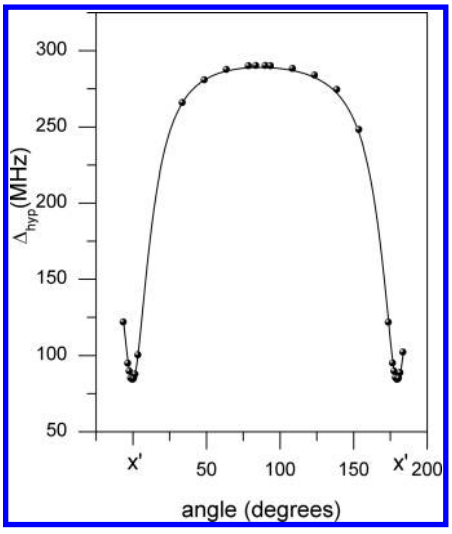

Figure 8. Hyperfine splitting Δ_{hyp} between the $m_I = \pm 1/2$ lines of the cobalt multiplet in the EPR spectrum of a single crystal of 1% $Co^{iPr,Ph}L_2/Zn^{iPr,Ph}L_2$ as a function of the orientation of the magnetic field in the same plane as in Figure 6. The dots represent the experimental observations and the line represents the fit based on eq 13, with $\Delta_{hyp} = 2\,[\Delta E^{+}(1/2)+\Delta E^{-}(1/2)]$.

shows that there is a small contribution to the line positions, quadratic in the nuclear spin quantum number. In this case, the splitting of the $m_I = \pm 1/2$ lines can be obtained from eq 13. From a least-squares fit of the variation of this splitting as a function of the orientation of $\vec{B}$ in the three planes (the same used for the analysis of the g′ tensor), the effective cobalt hyperfine tensor has

been derived. The fit showed that one of the principal axes of this tensor is parallel to the y′ axis, and this direction was fixed in the final fit. The quality of the description is illustrated for one plane in Figure 8. The principal values of the A′ tensor and the direction of the principal axes in the g′ tensor principal axes system are given in Table 1.

For $Co^{Ph,Ph}L_2$, the determination of the complete cobalt hyperfine tensor is hampered by the small values of g'_x and g'_y. Consequently, from the hyperfine splitting only $(A'_{z'x'}{}^2 + A'_{z'y'}{}^2 + A'_{z'z'}{}^2)^{1/2}$ can be extracted, for which a value of 222 MHz is found.

Discussion

The electronic structure of high spin (S = 3/2) Co(II) complexes is difficult to study by EPR because of the large ZFS of the spin sublevels. The complexes under study here, for which the cobalt is coordinated by four sulfur atoms, indeed have a substantial ZFS. For $Co^{Ph,Ph}L_2$ the magnitude of the ZFS (2 D′) amounts to 23.8 cm^{-1} (714 GHz) and for $Co^{iPr,Ph}L_2$ to 29.6 cm^{-1} (887 GHz). These splittings between the ±1/2 and ±3/2 doublets are much larger than the microwave quantum at the standard X-band EPR frequency (~9 GHz). Nevertheless, we have successfully applied EPR through the use of several microwave frequencies, variable temperatures, and single crystals.

$Co^{Ph,Ph}L_2$. For $Co^{Ph,Ph}L_2$, the ±3/2 doublet is found to be the lowest in energy, i.e., D is negative. The ZFS tensor is close to axial (λ = E/D ≈ − 0.05), and the transitions within the ±3/2 doublet, forbidden for E = 0, are correspondingly weak. The values of g'_x and g'_y are small and the EPR resonance field is largely determined by g'_z for many orientations of the magnetic field. The study of the EPR spectrum at X-band on a 1% $Co^{Ph,Ph}L_2$/$Zn^{Ph,Ph}L_2$ single crystal as a function of the orientation of the magnetic field shows that the principal z′ axis of the effective g tensor makes an angle of about 12° ± 3° with the crystallographic a axis. A comparable study for a 100% $Co^{Ph,Ph}L_2$ crystal resulted in a value of 6° ± 3° for this angle. The values of this angle are the same within experimental accuracy, but we can not exclude that the difference (partly) results from a slight deviation in the orientation of the Co complex with respect to the Zn complexes in the mixed crystal.

To discuss these EPR results, we consider the structure of $Co^{Ph,Ph}L_2$ as obtained from X-ray diffraction studies. The $Co^{Ph,Ph}L_2$ complex crystallizes in the P-1 space group with four molecules in the unit cell.[46] The CoS_4 core is made up by two bidentate (SPNPS) ligands with average endo P−S−Co−S torsion angles of about 20°. For zero torsion angles, the core would have D_{2d} symmetry. This is impossible because it would require planarity of the six-membered CoSPNPS rings. The nonplanarity of the ligands lowers the symmetry of the whole complex to approximately S_4, with the 4-fold improper rotation axis nearly along the N−N direction (Figure 1). The direction of the symmetry axis makes an angle of 3° with the crystallographic a axis. The $Co^{Ph,Ph}L_2$ and $Zn^{Ph,Ph}L_2$ complexes are isostructural,[48] and we assume that the description of the structure of the $Co^{Ph,Ph}L_2$ complex also applies to the structure of the complex in the mixed 1% $Co^{Ph,Ph}L_2$/$Zn^{Ph,Ph}L_2$ system, which we investigated in the EPR study.

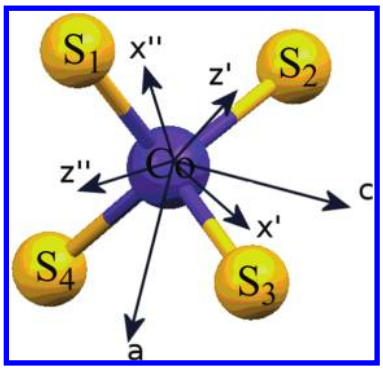

Figure 9. Orientation of the principal axes of the effective g tensor and of the A tensor in the CoS_4 core of $Co^{iPr,Ph}L_2$. The principal y′ and y″ axes, parallel to the C_2' axis and the crystallographic b axis, are normal to the plane of the paper. The directions of the crystallographic a and c axes are also shown.

The EPR results are consistent with the structural observations. The four molecules in the unit cell are magnetically indistinguishable, which corresponds to the fact that we have seen signals from one site only in the EPR spectra. The small but nonzero value of E agrees with the nearly S_4 symmetry of the $Co^{Ph,Ph}L_2$ complex. The z′ axis makes an angle of 12° ± 3° with the crystallographic a axis and of 20° ± 3° with the N−N direction. The close to S_4 symmetry implies that the principal z axes of g and D coincide in good approximation and eq 4 then reduces to $g'_z \approx 3\,g_z$. The value of 7.12 for g'_z translates to a value of about 2.37 for g_z. In this case also the principal z″ axis of the effective hyperfine tensor of cobalt will be along the symmetry axis. The observed effective cobalt hyperfine then corresponds to the principal value of the effective hyperfine interaction along the z″ direction, from which we obtain, according to eq 12, an absolute value of 74 MHz for the z″ component of the cobalt hyperfine interaction.

$Co^{iPr,Ph}L_2$. For $Co^{iPr,Ph}L_2$, the ZFS tensor is found to be rhombic ($\lambda \approx -0.33$). For E/D = ±1/3, the EPR spectra do not allow to determine the sign of the ZFS. Inverting the ±1/2 and ±3/2 doublets is equivalent to interchanging x and z (cf. eq 5 for $\theta = -15°$), and neither the fields of resonance nor the intensity of the transitions are affected. We note that we have not been able to resolve a second transition in the EPR spectra at higher temperatures, as we did for $Co^{Ph,Ph}L_2$. However, even if we could have performed an analysis similar to that for $Co^{Ph,Ph}L_2$, the determination of the sign of D would have been impossible. From the study of the EPR spectrum as a function of the orientation of the magnetic field with respect to a crystal, we have obtained the complete effective g tensor (Table 1 and Figure 9). The principal y′ axis is found to make an angle of 1° ± 3° degrees with the crystallographic b axis. In view of the small contribution of the Zeeman term, the x′,y′, and z′ axes represent not only the principal axes of the effective g tensor but also of the ZFS tensor.

The complex $Co^{iPr,Ph}L_2$ crystallizes in the $C2/c$ space group with four molecules in the unit cell.[47] Because the two phosphorus atoms in each CoSPNPS ring carry different substituents (a phenyl and an isopropyl group), the symmetry of the complex is lower than for $Co^{Ph,Ph}L_2$. Only one 2-fold rotation axis is left, which is indicated by

Table 3. Cobalt Hyperfine Tensor for $Co^{iPr,Ph}L_2$[a]

	$\|A_x\| = 127$	$\|A_y\| = 50$	$\|A_z\| = 107$
	x″	y″	z″
x′	−0.826	0	−0.563
y′	0	1	0
z′	0.563	0	−0.826

[a] The principal hyperfine values are given in MHz. The orientation of the principal axes x″,y″,z″ of the A tensor is represented by their direction cosines in the axes system x′,y′,z′ of the effective g tensor.

C_2' as it is perpendicular to the S_4 axis of the core (Figure 1). The C_2' axis bisects the exo S−Co−S angles and is parallel to the crystallographic b axis. The complex adopts the so-called "bird-arrangement",[54,55] and its structure is close to that of the FeS_4-site found in the active center of desulforedoxine.[56] We assume that the $Co^{iPr,Ph}L_2$ complex has the same structure in the mixed 1% $Co^{iPr,Ph}L_2/Zn^{iPr,Ph}L_2$ crystal as in the pure crystal.

One of the principal axes of the effective g tensor, the y′ axis, virtually coincides with the crystallographic b axis (cf. Table 1), which is consistent with the symmetry of the complex. One of the principal axes should be parallel to C_2', and the C_2' axis is indeed parallel to the b axis. The y′ axis and one of the principal axes of the D tensor coincide along C_2', and from $g'_y = 2.38$ and $\lambda = -0.33$ we obtain $g_y = 2.38$. The other principal axes of the g and D tensors might well be rotated with respect to each other, a fact that prohibits the determination of g_x and g_z from the corresponding effective g values. The principal axes of the effective g tensor and of the effective cobalt hyperfine tensor virtually coincide. The cobalt hyperfine tensor can be determined from the effective tensor according to eq 12. The principal values and the direction of the principal axes are presented in Table 3 (Figure 9). One of the principal axes, the y″ axis, is for symmetry reasons parallel to the y′ axis, while x″ and z″ are found to be rotated by 34° with respect to x′ and z′. Unfortunately, a further interpretation of the cobalt hyperfine interaction is as yet impossible, because only the absolute value of the tensor elements is known. The signs could not be determined from the EPR data, because the contribution of the nuclear Zeeman interaction to the hyperfine splitting is too small.

In the next paragraphs we discuss our results in relation to EPR reports on cobalt coordination in the literature. Of particular interest is a series of papers by Fukui et al.[34−36] in which they reported on Co-thiolate coordination as studied by variable-temperature magnetic susceptibility measurements and low-temperature X-band EPR experiments. They investigated $[Co^{II}(SR)_4]A_2$ type of complexes, where R = (substituted) phenyl and the counterion A = $[N(CH_3)_4]^+$, $[N(C_2H_5)_4]^+$, or $[P(C_6H_5)_4]^+$. From experiments on powder samples, largely different ZFS values have been reported, even when only the counterion is different.[36] The parameter D′ was found to vary between 2 and 100 ± 30 cm^{-1}, and the parameter λ varied between −0.21 and 0.19, which implies a change in the order of the levels of the Kramers doublet. Two subsequent papers described more detailed investigations of single crystals of two of the complexes.

For $[Co(SPh)_4]$ $[P(Ph)_4]_2$,[37] a complex of approximate D_{2d} symmetry, the ZFS parameters have been reported as $D = -70 \pm 10$ cm^{-1} and $|\lambda| < 0.09$, and the effective g values as < 0.6, < 1.5, and 7.75 ± 0.1. Only upper limits of the lowest g′ values could be determined because the EPR experiments were limited to X-band frequency and magnetic fields below 1 T. Comparison with the data for $Co^{Ph,Ph}L_2$, a complex of approximate S_4 symmetry, shows that the effective g values are similar (0.3, 0.3, and 7.12), while the D value is negative as well but much smaller (-11.9 ± 0.2 cm^{-1}).

For $[Co(SPh)_4]$ $[N(CH_3)_4]_2$,[38] the ZFS parameters have been reported as $D' = 6.5$ cm^{-1} and $\lambda = 0.30$. Fukui et al. describe the symmetry of this complex as approximately S_4, which seems to be at variance with the rhombicity of the zero-field splitting. The conclusion as regards the positive sign of D is based on the analysis of the principal g′ values but, as shown above, cannot be conclusive because of the value of λ being close to 1/3. The principal g′ values found for this complex are 1.64, 2.34, and 5.68, similar to the values we obtained for $Co^{iPr,Ph}L_2$ (1.62, 2.38, and 6.44), and compatible with both negative and positive D, which leaves the order of the Kramers doublets undetermined. Besides the largest g′ value, also the magnitude of D′ (14.8 cm^{-1}) is bigger for $Co^{iPr,Ph}L_2$ than for the rhombic $[Co(SPh)_4]^{2-}$ complex.

Whether the magnitude of the ZFS of four-coordinated high-spin Co(II) complexes varies largely, remains to be seen. For the $Co^{Ph,Ph}L_2$ and $Co^{iPr,Ph}L_2$ complexes the Kramers doublets are about 24 and 30 cm^{-1} apart (values of 2D′). An accurate value of the splitting has also been reported for $Co(PPh_3)_2Cl_2$, and is of comparable size. It amounts to 29 cm^{-1}, as derived from HFEPR and VTVH-MCD.[39]

Combining the observations on all complexes with a CoS_4 core indicates that subtle structural variations are attended with significant changes of the electronic level structure. For the $[Co(SPh)_4]^{2-}$ complexes, the structural variations are induced by changing the counterion, whereas for the complexes studied here by a change in the substituent at the phosphorus atoms in the bidentate ligand. In both cases, a change in the S−Co−S−X (X = C or P) torsion angles seems to be involved. Fukui et al.[38] concluded that the large variation of the level structure in zero field derives from a strong dependence of the spin−orbit coupling between the $^4T_2$ excited state and the $^4A_2$ ground state on the S−Co−S−C torsion angles. This dependence in turn has been described in relation to the variation in the σ- versus π-character of the Co−S bonds. In retrospect, their conclusions may have been premature, being based upon incomplete data and interpretations, but are interesting and stimulate further study.

For $Co^{iPr,Ph}L_2$ we have derived the complete cobalt hyperfine tensor, which to the best of our knowledge presents the first such result for (distorted) tetrahedral cobalt complexes. Previously, cobalt hyperfine splitting was resolved for powders or solutions in a few cases, mostly limited to the low-field EPR transition. This concerns cobalt sites in which the cobalt is coordinated

(54) Vrajmasu, V. V.; Bominaar, E. L.; Meyer, J.; Munck, E. *Inorg. Chem.* **2002**, *41*, 6358–6371.
(55) Vrajmasu, V. V.; Munck, E.; Bominaar, E. L. *Inorg. Chem.* **2004**, *43*, 4867–4879.
(56) Archer, M.; Huber, R.; Tavares, P.; Moura, I.; Moura, J. J. G.; Carrondo, M. A.; Sieker, L. C.; Legall, J.; Romao, M. J. *J. Mol. Biol.* **1995**, *251*, 690–702.

to sulfur, nitrogen, and/or oxygen.[37,57−59] Only the effective hyperfine coupling can be derived, and the scarce data do not allow a systematic comparison as yet.

In conclusion, the application of EPR spectroscopy in a broad range of magnetic fields and microwave frequencies has been found most suitable in the study of complexes with a pseudotetrahedral CoS_4 core. The EPR experiments reveal that the Kramers doublets of $Co^{Ph,Ph}L_2$ and $Co^{iPr,Ph}L_2$ are 24 and 30 cm^{-1} apart in zero magnetic field. In that sense the complexes are found to be similar, but the EPR spectra are very different. This results from the fact that the ZFS is close to axial for $Co^{Ph,Ph}L_2$ and rhombic for $Co^{iPr,Ph}L_2$, in agreement with the different symmetry of the complexes, which is determined by subtle differences in the "second" coordination sphere of the CoS_4 cores. Different microwave frequencies have been employed in the EPR experiments, the largest one being 275 GHz, which corresponds to about 9 cm^{-1}. This means that we have by far not reached the situation that the Zeeman contribution dominates the ZFS, which complicated the interpretation of the spectra. We have nevertheless successfully analyzed the spectra through the use of variable low temperatures, fine powder samples, and (diamagnetically diluted) single crystals. In this way the contributions to the spectra of the ZFS, the Zeeman interaction, and the cobalt hyperfine interaction have been separated. Complete effective g and cobalt hyperfine tensors have been obtained, including the principal values and the directions of the principal axes in the cobalt sites. Because these experiments were performed under the condition of a very small Zeeman contribution, the directions of the principal axes of the effective g tensor also represent those of the ZFS tensor.

To be able to fully describe the electronic properties of the $Co^{Ph,Ph}L_2$ and $Co^{iPr,Ph}L_2$ complexes, more data are necessary. Toward this goal we presently extend our investigations to electron−nuclear double resonance experiments, to probe the delocalization of the electronic wave function over the ligand.[60] In parallel, density-functional-theory and ab initio multireference calculations are currently being applied, which are expected to further elucidate the electronic structure of these systems. The accurate values of the ZFS and the cobalt hyperfine interaction obtained in this work for two CoS_4-containing complexes provide important reference data for such a theoretical approach.

Acknowledgment. We acknowledge the assistance of Dr. H. Blok and Dr. P. Gast in the EPR experiments. We thank Dr. A.A.M. Schreurs (Utrecht University, The Netherlands) for the X-ray diffraction measurements. The part of this research performed at Leiden University is financially supported by The Netherlands Organization for Scientific Research (NWO-CW). D.M. thanks the European Commission Research Directorates (Marie Curie fellowship grant HPM-CT-2000-00120) for the opportunity to work at Leiden University. P.K. acknowledges the Special Account of the University of Athens (grant 70/4/7575) and the Empirikion Foundation for funding. Dr. Alexios Grigoropoulos is thanked for helpful discussions.

Supporting Information Available: Figure S1 showing $^{31}P\{^1H\}$ NMR and UV−vis spectra of $Co^{Ph,Ph}L_2/Zn^{Ph,Ph}L_2$ at various percentages; Figure S2 showing cw EPR spectra of $Co^{Ph,iPr}L_2$ obtained in various solvents; Figure S3 showing a cw-EPR spectrum of a single crystal of 1% $Co^{Ph,Ph}L_2/Zn^{Ph,Ph}L_2$. This information is available free of charge via the Internet at http://pubs.acs.org.

(57) Makinen, M. W.; Yim, M B. *Proc. Natl. Acad. Sci.* **1981**, *78*, 6221–6225.
(58) Bennet, B. *Curr. Top. Biophys.* **2002**, *26*(1), 49–57.
(59) Horrocks, W. D.; Ishley, J. N.; Holmquist, B.; Thompson, J. S. *J. Inorg. Biochem.* **1980**, *12*, 131–141.
(60) Sottini, S.; Mathies, G.; Gast, P.; Maganas, D.; Kyritsis, P.; Groenen, E. J. J. *Phys. Chem. Chem. Phys.* **2009**, *11*, 6727–6732.